JOURNAL OF SOLID STATE CHEMISTRY 26, 265–274 (1978)

Electrical Properties of the α, β, γ, and δ Phases of Bismuth Sesquioxide

H. A. HARWIG* AND A. G. GERARDS

Inorganic Chemistry Department, State University Utrecht, Croesestraat 77A, Utrecht, The Netherlands

Received February 1, 1978

Conductivity measurements have been performed on compressed powder specimens of Bi_2O_3 in the temperature region 300–800°C. The conductivity in the β, γ, and δ phases is predominantly ionic. Oxide ions are the mobile charge carriers. The disorder in these phases is intrinsic even when the samples are contaminated with Au or Pt. The conductivity in the α phase is predominantly p type. The disorder in the α phase is extrinsic up to the $\alpha \rightarrow \delta$ transition at 729°C. From 650 to 729°C a rapidly increasing contribution of oxygen vacancies to the conductivity is apparent.

Introduction

The polymorphism of Bi_2O_3 was recently investigated by the present authors (*1*). The monoclinic α phase is the stable phase at room temperature. At 729°C a transition occurs to the high-temperature *fcc* δ phase, which is stable up to the melting point at 824°C. On cooling from the δ phase thermal hysteresis was observed over 80–90°C. The δ phase transforms to the α phase via one of two intermediate phases. Either the tetragonal β phase is formed at 650°C or the *bcc* γ phase is formed at 639°C. The intermediate phases showed a fast transition to the α-phase at arbitrary temperature in the region 650–490°C. The γ phase persisted to room temperature in some experiments.

Limited information is available on the electrical properties of Bi_2O_3. Mansfield (*2*) and Hauffe and Peters (*3*) observed p-type conduction in α-Bi_2O_3 which changed into n-type conduction above 550°C at oxygen pressures below 1.3×10^{-5} atm. Rao *et al.* (*4*) suggested that n-type conduction occurs above 650°C even in air. They assumed that the conduction in α- and δ-Bi_2O_3 is electronic and ascribed the increase in the conductivity at the $\alpha \rightarrow \delta$ transition to the broadening of the bands in Bi_2O_3. To the contrary, Takahashi *et al.* (*5*) reported that in the high-temperature δ phase oxide ions are the major charge carriers. An increase in the conductivity of approximately 3 decades was observed at the phase transition from the electronic-conducting α phase to the high-ionic-conducting δ phase. Takahashi and co-workers (*5–12*) investigated the conductivity of mixed oxides in the systems Bi_2O_3–M_xO_y (M = Sr, Ca, La, W, Y, Gd, Ba, Mo). Several solid solutions in these systems show high ionic conductivity.

The present authors (*1*) reported the existence regions of the intermediate phases, among others, on the basis of preliminary conductivity measurements performed during cooling from the liquid state. Details of the conductivity in the intermediate phases have not been reported yet. In view of the high ionic

* Author to whom correspondence should be addressed.

0022-4596/78/0263-0265$02.00/0

conductivity in the δ phase and the structural relations between the various phases (*13*), we decided to investigate the electrical conductivity in the various phases of Bi_2O_3.

Experimental

Bismuth sesquioxide (Kawecki–Billiton, 99.99% pure) was used as the starting material. Spectrochemical analysis showed that Si (0.001 wt%) was the main impurity. Except for Fe (0.0002 wt%) and Mg (0.00005 wt%) no metals could be detected. Pellets with diameters of 0.8 cm and thicknesses in the range 0.3–0.8 cm were pressed in a stainless steel die with 1000 kg cm^{-2}. The pellets were sintered for 24 hr in air at 670°C, i.e., below the $\alpha \rightarrow \delta$ transition temperature. After sintering, the apparent density of the samples was approximately 85% of the theoretical density. The flat faces of the pellets were covered with Au paint (Louyot OC/17) or Pt paint (Degussa Leitplatin). After firing at 600°C, satisfactory electrode contacts were obtained. The samples had the characteristic light yellow color of α-Bi_2O_3. The samples were spring loaded between Au or Pt foil in a quartz or stainless steel (*14*) conductivity cell. By passing mixtures of nitrogen and oxygen through the cells the gas atmosphere could be adjusted. In view of the metastability of the intermediate phases special precautions were taken to minimize temperature fluctuations. To detect the phase transitions the temperature was varied continuously with 1°C min^{-1}. At regular intervals it was checked, by isothermal measurements, whether equilibrium had been reached. The temperature of the sample was measured by means of a thermocouple with the junction at 0.05 cm from the sample.

The conductivity was measured in the temperature range 300–800°C with a Wayne–Kerr B641 autobalance bridge (1592 Hz) equipped with an automatic ranging system. If the conductivity exceeded 0.1 Ω^{-1}, a four-wire arrangement was used. The conductivity at the bridge frequency of 1592 Hz differed only slightly from the high-frequency limit of the conductance, the true bulk conductivity. The conductivity and the temperature of the sample were recorded continuously during the experiments.

Measurements of the admittance were performed in the frequency range 60 kHz–3 mHz. Alternating currents of 100 μA to 1 mA were passed through the sample under galvanostatic conditions. The voltage response across the sample and the reference signal were amplified with a matched pair of Tektronix AM502 differential amplifiers. In the frequency range 60 kHz–2 Hz the in-phase and quadrature components were measured with a Brookdeal 9502 two-phase lock-in amplifier. Below 2 Hz the admittance parameters were determined by the analysis of Lissajous figures displayed on an XY recorder.

To determine the dc conductivity, direct currents of 10 μA–10 mA were applied under galvanostatic conditions. Galvanostatic current steps of 10-min duration were used to investigate the presence of low-frequency dispersion in the admittance. Direct currents were passed for several hours through some samples to establish the nature of the ionic charge carriers. The maximum charge passed was 29 C.

Results

Conductivity measurements on samples with Pt and Au electrodes gave essentially the same results. In Fig. 1 some typical plots of $\log \sigma - 1/T$ for $Pt|Bi_2O_3|Pt$ are presented, which were obtained during repeated heating and cooling runs. The conductivity increases over 3 decades at the $\alpha \rightarrow \delta$ transition at 729°C. In the cooling direction a hysteresis of 80 or 90°C precedes the transition to the intermediate β or γ phase, respectively. In the various cooling runs one of these phases appeared in arbitrary order as in the differential thermal analysis reported previously (*1*). The transitions from the metastable inter-

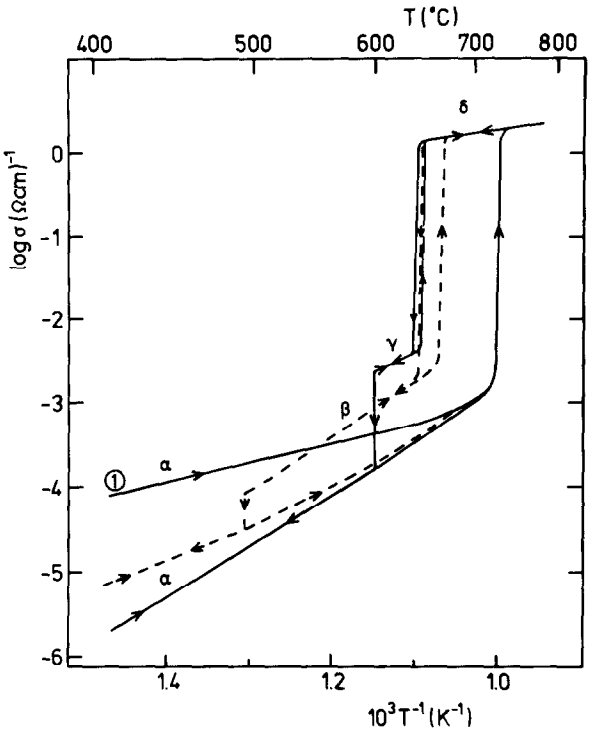

FIG. 1. Some typical plots of the logarithm of the conductivity σ versus T^{-1} for Pt|Bi_2O_3|Pt in air, showing the existence regions of the various phases. The measurements were performed at 1592 Hz. For the sake of clarity the measurement in which the β phase appeared is presented by a broken line. (1) Starting measurement.

mediate phases to the α phase occurred at arbitrary temperature. These transitions proceeded very rapidly, as was inferred from the sharp peak on the temperature–time line of the sample. In some experiments the γ phase persisted to room temperature. In the measurements with Pt electrodes the transitions $\delta \leftrightarrow \beta$ and $\delta \leftrightarrow \gamma$ showed some hysteresis, as can be seen from Fig. 1. The transition $\delta \rightarrow \beta$ proceeds considerably faster than the $\delta \rightarrow \gamma$ transition. The $\delta \rightarrow \beta$ and the $\delta \rightarrow \gamma$ transitions manifested themselves in the temperature–time line by a peak and a small plateau, respectively. The transition temperatures observed in the conductivity measurements compare well with our previous results (*1*) of differential scanning calorimetry (see Table I).

In the experiments with Au electrodes a gradual decrease of the conductivity of samples in the δ phase preceded the actual $\delta \rightarrow \gamma$ transition. Since the effect was very sluggish it was investigated by isothermal measurements. In Fig. 2 the high-frequency limits of the conductance are given in a plot of $\log \sigma - 1/T$. In the region 664–640°C a rapid decrease in conductivity was observed in the δ phase, followed by a transition to the γ phase. Heating

TABLE I

TRANSITION TEMPERATURES IN Bi_2O_3 FROM CONDUCTIVITY MEASUREMENTS AND DIFFERENTIAL SCANNING CALORIMETRY (*1*)

Transition	Temperature (°C)	
	σ	DSC
$\alpha \rightarrow \delta$	729	730(1)
$\delta \rightarrow \beta$	648	649(2)
$\beta \rightarrow \delta$	663	667(1)
$\delta \rightarrow \gamma$	641	643(2)
$\gamma \rightarrow \delta$	650	652(2)

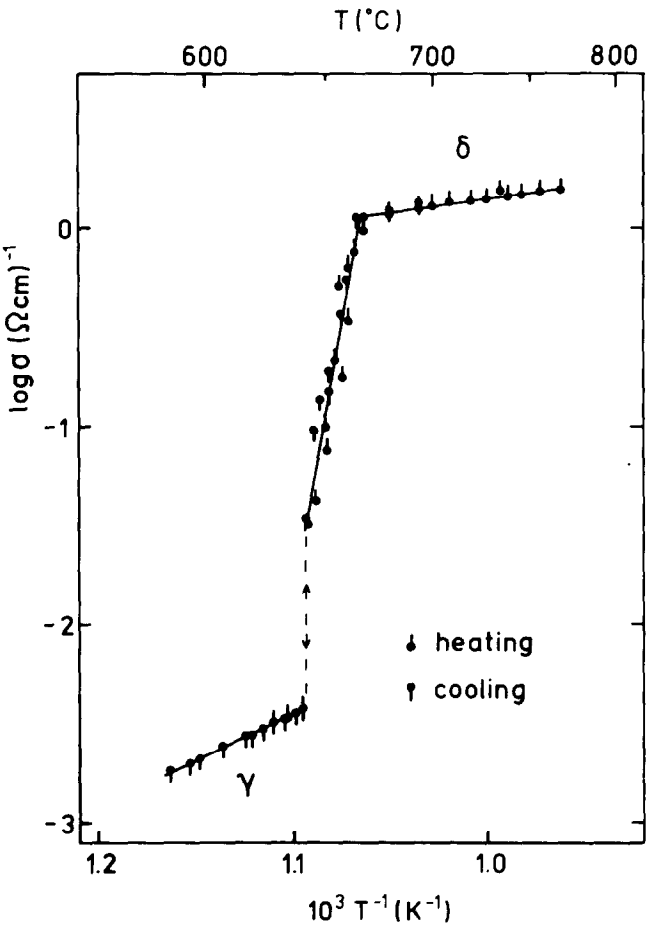

FIG. 2. The conductivity σ of a specimen Au | Bi_2O_3 | Au in air from the high-frequency limits of the conductance, plotted as log σ versus T^{-1}.

from the γ phase, the δ phase showed a corresponding rapid increase in conductivity. No hysteresis was observed. The activation enthalpy calculated from a plot of log $\sigma T - 1/T$ is about 10 eV in the temperature region 640–664°C. Equilibrium was attained about 1 hr after a temperature step of 3°C. Isothermally the conductivity remained constant for 40 hr at least. The most likely explanation for this behavior is the occurrence of ordering in the defect fluorite structure of δ-Bi_2O_3 (*13*).

The conductivity of the β, γ, and δ phases was measured reproducibly in various heating and cooling runs and on different samples. The conductivity was independent of the electrode material employed. To the contrary, the conductivity in the α phase of samples cooled from the δ phase increased if Au was used, but decreased if Pt was used as electrode material (see Fig. 1). The samples that were cooled from the δ phase and were supplied with Au or Pt electrodes were brown or grey in color, respectively. In Fig. 3 the conductivity of a stack of three Bi_2O_3 pellets between Au electrodes is compared with the conductivity of the pellet which was situated adjacent to one of the Au electrodes. This clearly demonstrates the increase in conductivity with increasing content of dissolved Au. The

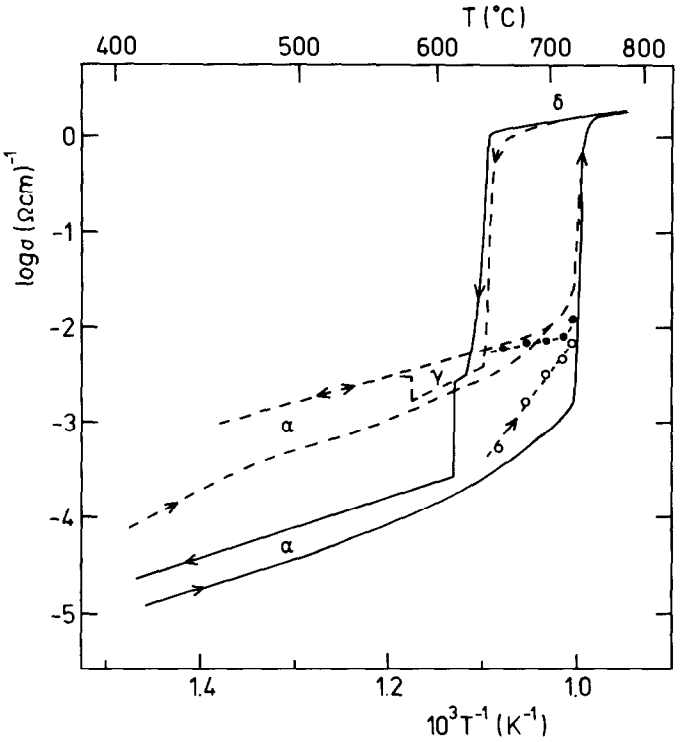

Fig. 3. The conductivity σ (1592 Hz) of Au|Bi_2O_3|Au in air plotted as log σ versus T^{-1} (see text). Straight line: stack of three pellets; broken line: pellet adjacent to the Au electrode; open circles: ionic contribution to the maximum conductivity of the α phase; closed circles: contribution of holes to the maximum conductivity of the α phase.

increase in the conductivity of the pellet adjacent to the Au electrode with respect to the conductivity measured in the first heating run of this single pellet can be explained by the homogenization of dissolved Au in the oxide in the δ phase. This is substantiated by the observation that the pellet was homogeneously colored after the experiment, whereas it exhibited a colored band next to the electrode when it was separated from the stack. The maximum conductivity in the α phase as given in Fig. 3 was never exceeded in our measurements, and it seems to be related to a maximum in the Au dissolution. Emission spectroscopical analysis of the homogeneously brown-colored samples which exhibited this conductivity revealed an Au content of 0.06 wt%. Samples supplied with Pt electrodes contained 0.04–0.06 wt% of Pt after a series of measurements.

In the δ phase frequency dispersion was observed in the admittance from 60 kHz to 3 mHz in accordance with the high ionic conductivity in this phase. Figure 4 presents some typical impedance plots in the complex plane representation for the cell Au|δ-Bi_2O_3|Au in air. Analysis of the admittance data shows that this dispersion is caused by diffusion of oxygen to the electrode/electrolyte interphase. Details will be published elsewhere (*15*). The conductivity in the δ phase was independent of the oxygen partial pressure at least down to 10^{-8} atm. In the intermediate β and γ phases frequency dispersion was encountered at lower frequencies, presumably because of the lower conductivity of the electrolyte. Figure 5 presents some impedance plots in the complex plane representation for the cell Au|γ-Bi_2O_3|Au in air. Down to 40–10 mHz, depending on the temperature, dif-

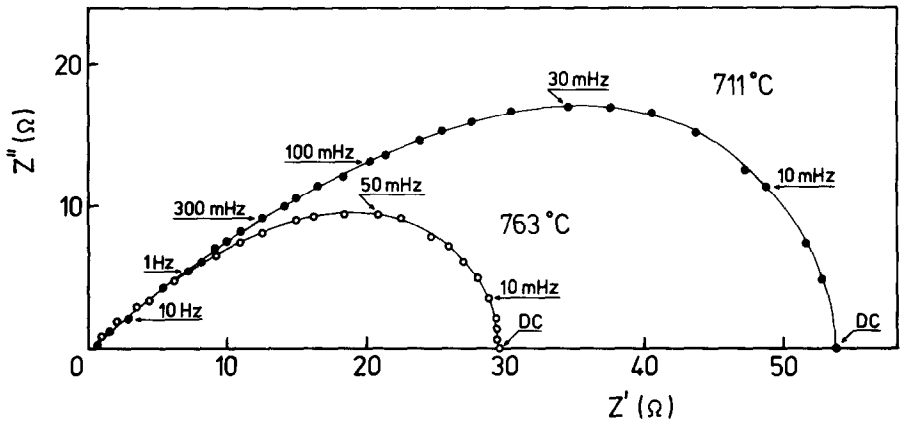

FIG. 4. Impedance plots for the cell Au | δ-Bi_2O_3 | Au in air.

fusional (Warburg) behavior is observed. Deviations are present below these frequencies, since the diffusion occurs over the limited distance of the adsorption site on the Au particles or the electrolyte surface to the actual electrode/electrolyte interphase (*15*). The aforementioned results indicate that the conduction is predominantly ionic in the β, γ, and δ phases. The activation enthalpies calculated from a plot of $\log \sigma T - 1/T$ are 1.37, 0.98, and 0.40 eV for the β, γ, and δ phases, respectively.

No frequency dispersion in the frequency region involved could be detected in the α phase below 650°C, which indicates that the α phase is predominantly electronic conducting below this temperature. Galvanostatic current steps of 100 μA and 10-min duration were passed through a sample in the α phase with a high Au content in the temperature region 650–729°C. The voltage response immediately after the start of the current step corresponded with the admittance of the

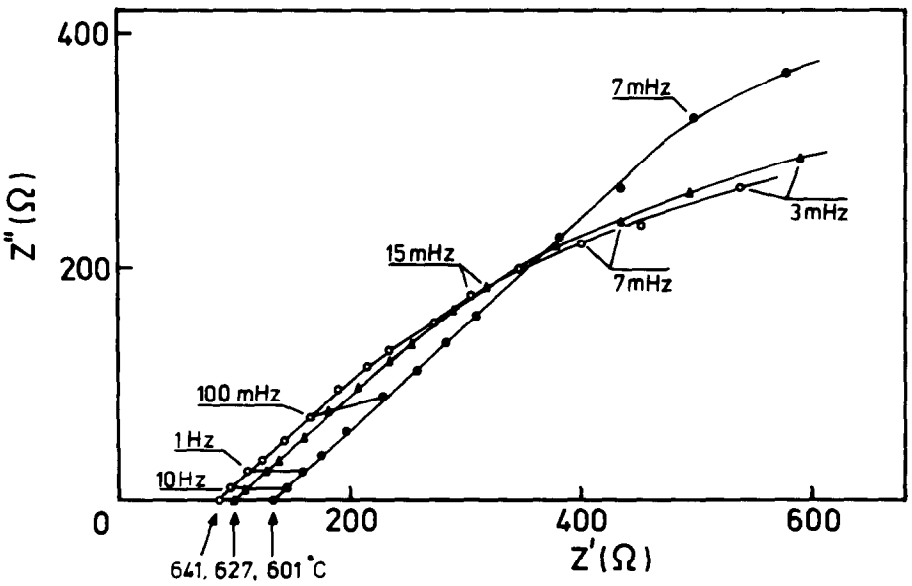

FIG. 5. Impedance plots for the cell Au | γ-Bi_2O_3 | Au in air.

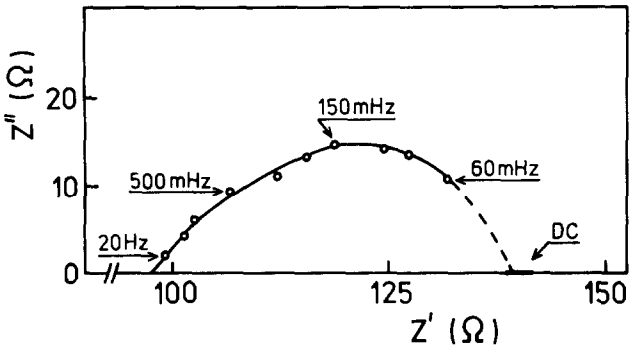

Fig. 6. Impedance plot for the cell Au|α-Bi_2O_3|Au in nitrogen with 500 ppm of oxygen at 676°C.

sample at 1592 Hz. At 676°C in air a constant voltage was reached after 3 min, indicating interphase polarization, although no complex plane impedance diagram could be determined in these circumstances. In a nitrogen atmosphere containing 500 ppm of oxygen, low-frequency impedance data could be obtained (see Fig. 6), which indicates a lower electronic contribution to the total conductivity at lower oxygen partial pressures. The conductivity of the α phase was measured as a function of the oxygen partial pressure in the temperature range 650–729°C. In Fig. 7 the conductivity is plotted versus $P_{O_2}^{0.25}$.

After the transport experiments we did not find morphological changes in the specimens or electrodes which are expected if transport of bismuth ions occurs. No blocking occurred during the transport experiments when direct currents of 1 mA were passed through the samples for several hours. Therefore the major contribution to the ionic conductivity in the various phases is attributed to the transport of oxide ions.

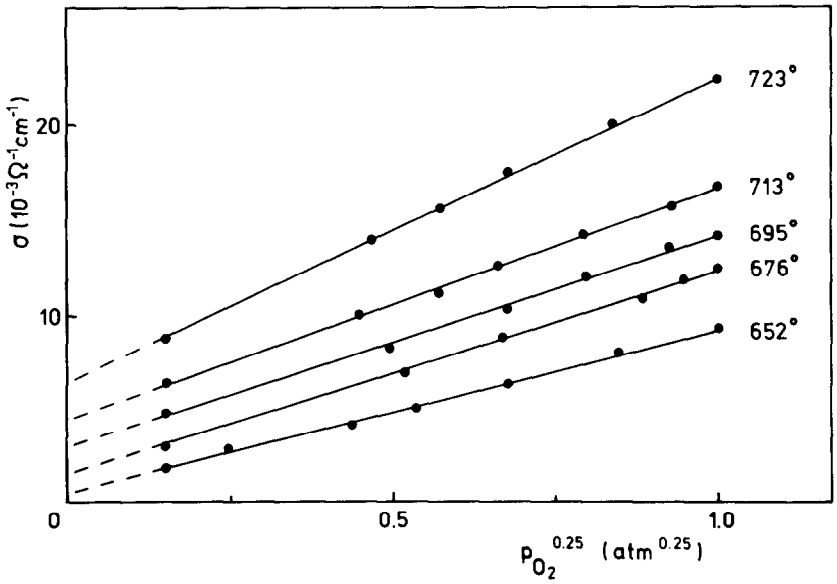

Fig. 7. Conductivity σ for Au|α-Bi_2O_3|Au from the high-frequency limits of the conductance, plotted as σ versus $p_{O_2}^{0.25}$. Temperatures are indicated in degrees Celsius.

Discussion

The conductivity in the β, γ, and δ phases of Bi_2O_3 was measured reproducibly for different samples, although the samples became progressively contaminated with aliovalent metal ions from the electrode material. Therefore the disorder in these phases is intrinsic. The disorder responsible for the conductivity in the α phase is clearly not intrinsic.

The present results show that δ-Bi_2O_3 exhibits high ionic conductivity with oxide ions as the mobile charge carriers. This is in agreement with the results of electromotive force and transport measurements by Takahashi *et al.* (*5*). The high intrinsic disorder and the high mobility of the oxide ions are in accordance with the entropy and the structure of δ-Bi_2O_3. The gain in entropy at the $\alpha \rightarrow \delta$ transition is 75% of the overall gain in entropy from the α phase to the liquid state (*1*). The disorder in the δ phase is therefore comparable to that in the liquid state. The disorder can be ascribed to the liquid-like behavior of the oxygen sublattice, as was deduced from high-temperature neutron diffraction experiments (*16*). Our previous measurements (*1*) revealed that the conductivity in the δ phase is comparable to that in the liquid state. Comparison of theoretical and experimental electromotive forces (*18*) showed that the conduction in molten Bi_2O_3 is mainly ionic. The effect of ordering in the oxygen sublattice of the δ phase could not be established with the diffraction experiments. The ordering phenomena seem to be influenced by the presence of impurities and need further investigation. The effect might be related to the long-range order at 1100°C in the oxygen sublattice of calcia-stabilized zirconia observed by Carter and Roth (*17*).

The structures of α-, β-, and γ-Bi_2O_3 can be described as distorted defect fluorite structures (*13*). Space and electrostatic considerations indicate that, in principle, Frenkel disorder is possible in the anion sublattice of the α and β phases (*13*). Whether the oxygen sublattice of the γ phase is occupied completely is not certain at present. On structural grounds Frenkel disorder seems possible in the oxygen sublattice of the γ phase (*13*).

Small electronic contributions (<1%) to the conductivity of the β, γ, and δ phases are hard to detect, since no true blocking electrodes for oxygen are available at present at the high temperatures involved. Recently Takahashi *et al.* (*11*, *12*) reported the determination of the electronic contribution to the conductivity of the solid solution $(Bi_2O_3)_{0.73}(Y_2O_3)_{0.27}$ by means of polarization measurements using a glass-coated Ag electrode. The ionic conductivity in air (500–700°C) of this fcc material is at least two orders of magnitude higher than the hole conductivity and five orders higher than the electron conductivity.

The conductivity in the α phase is mainly electronic. In agreement with the results of Mansfield (*2*), we observed that in α-Bi_2O_3, $\sigma \sim p_{O_2}^{0.25}$. Since the electronic conductivity increases with oxygen pressure holes are the main charge carriers (*19*). From 650 to 729°C mixed ionic–electronic conduction was observed in the α phase. Since the *p*-type conductivity of α-Bi_2O_3 increases with increasing Au content and decreases with increasing Pt content, the impurities are most likely incorporated substitutionally on bismuth sites as Au^+ or Au^{2+} or as Pt^{4+}, respectively. Recently de Wit (*20*) described the defect chemistry of In_2O_3. The derived oxygen pressure dependence of the various defect concentrations can be used for Bi_2O_3. The results for uni- and divalent dope are essentially the same and the discussion will be confined here to divalent gold as the impurity. The defect notation of Kröger is used (*19*).

In principle a Schottky defect situation, Frenkel disorder in the anion sublattice, or Frenkel disorder in the cation sublattice may predominate in α-Bi_2O_3. The choice among these models is irrelevant for the qualitative aspects. From low to high oxygen pressure, four regions are encountered (*20*). In the first region the disorder is intrinsic. In the second region the concentrations of the ionic point

defects are impurity controlled. For the hole concentration $p \sim p_{O_2}^{0.25}[Au'_{Bi}]^n$, where $n = \frac{1}{2}$ for the Schottky defect situation or Frenkel disorder in the anion sublattice and $n = \frac{1}{3}$ for Frenkel disorder in the cation sublattice. In this region the hole conductivity will depend on both the oxygen pressure and the impurity concentration. In the third region the hole conductivity is impurity controlled, since $p = [Au'_{Bi}]$. In the fourth region the disorder is again intrinsic. Our experimental results for the α phase, i.e., increasing conductivity with increasing Au content and $\sigma \sim p_{O_2}^{0.25}$, are in accordance with the behavior expected in the second region. In this region the concentrations of oxygen vacancies and interstitial oxygen are controlled by the impurity concentration, i.e., $[V_{\ddot{O}}] \sim [Au'_{Bi}]^m$ and $[O''] \sim [Au'_{Bi}]^{-m}$, where $m = 1$ for the Schottky defect situation or Frenkel disorder in the anion sublattice and $m = \frac{2}{3}$ for Frenkel disorder in the cation sublattice. Therefore the ionic conductivity in this region is independent of the oxygen partial pressure.

For intermediate oxygen pressures the total conductivity in the α phase can be described by

$$\sigma = \sigma_h^0 p_{O_2}^{0.25} + \sigma_O.$$

where σ_h^0 and σ_O denote the conductivity due to holes (at $p_{O_2} = 1$ atm) and to oxide ions, respectively. In Fig. 7 the high-frequency limits of the conductance in the α phase in the temperature region 650–729°C are plotted versus $p_{O_2}^{0.25}$. The slope of this plot represents σ_h^0. The ionic conductivity σ_O can be found by extrapolation of the conductivity to zero oxygen pressure. Accurate data can be obtained in this way, provided the hole and ionic conductivities are of the same order. The contributions of holes and oxide ions to the maximum conductivity in the α phase in air are shown in Fig. 3.

Since the total conductivity of a nominally pure sample is lower than the oxide ion conductivity of a sample contaminated with gold (see Fig. 3), it is clear that the oxide ion conductivity increases with increasing Au content. This is possible only if oxygen vacancies are the mobile ionic charge carriers ($[V_{\ddot{O}}] \sim [Au'_{Bi}]^m$). The ionic conductivity in α-Bi_2O_3 shows a steep increase near the transition to the δ phase with an activation enthalpy of 2.7 eV calculated from a plot of $\log \sigma T - 1/T$. Since the defect concentration is determined by the amount of impurity this steep increase can be ascribed to the breakdown of associates in which oxygen vacancies participate or by a fast increase of the mobility of oxygen vacancies. The latter explanation implicates an increase in the disorder in the oxygen sublattice preceding the actual phase transition to the δ phase.

The changes in the slope of the conductivity versus reciprocal temperature for α-Bi_2O_3 at ± 580°C ($p_{O_2} = 2.6 \times 10^{-4}$ atm) and 650°C ($p_{O_2} = 0.2$ atm) observed by Rao *et al.* (*4*) agree with our observations. In view of the foregoing this effect should not be ascribed to a change from *p*-type to *n*-type conduction, as proposed by Rao *et al.*, but to an increase of the contribution of oxide ions to the total conductivity.

Conclusions

The conductivity in the β, γ, and δ phases of Bi_2O_3 is mainly ionic. Oxide ions are the mobile charge carriers. The disorder in the β, γ, and δ phases is intrinsic. The ionic conductivity in the δ phase, which has a disordered partially occupied oxygen sublattice, is about three orders of magnitude higher than the conductivity in the intermediate phases. The α phase is predominantly electronic conducting in the temperature range 400–729°C. Holes are the mobile charge carriers. The disorder in the α phase is extrinsic up to the $\alpha \rightarrow \delta$ transition. From 650 to 729°C a rapidly increasing contribution of oxygen vacancies to the conductivity is apparent.

Acknowledgments

The authors are indebted to Prof. Dr. W. van Gool for encouraging this work. Dr. R. W.

Bonne of the Solid State Chemistry Department of this University is gratefully acknowledged for valuable discussions during the preparation of the manuscript. Thanks are due to Mr. Bastings of the Philips Research Laboratories (Eindhoven, The Netherlands) for the emission spectroscopical analyses. The present investigations have been carried out under the auspices of the Netherlands Foundation for Chemical Research (SON) with financial aid from the Netherlands Organization for the Advancement of Pure Research (ZWO).

References

1. H. A. HARWIG AND A. G. GERARDS, *Thermochim. Acta*, in press.
2. R. MANSFIELD, *Proc. Phys. Soc. London B* **62**, 476 (1949).
3. K. HAUFFE AND H. PETERS, *Z. Phys. Chem.* **201**, 121 (1952).
4. C. N. R. RAO, G. V. SUBBA RAO, AND S. RAMDAS, *J. Phys. Chem.* **73**, 672 (1969).
5. T. TAKAHASHI, H. IWAHARA, AND Y. NAGAI, *J. Appl. Electrochem.* **2**, 97 (1972).
6. T. TAKAHASHI AND H. IWAHARA, *J. Appl. Electrochem.* **3**, 65 (1973).
7. T. TAKAHASHI, H. IWAHARA, AND T. ARAO, *J. Appl. Electrochem.* **5**, 187 (1975).
8. T. TAKAHASHI, T. ESAKA, AND H. IWAHARA, *J. Appl. Electrochem.* **5**, 197 (1975).
9. T. TAKAHASHI, T. ESAKA, AND H. IWAHARA, *J. Solid State Chem.* **16**, 317 (1976).
10. T. TAKAHASHI, T. ESAKA, AND H. IWAHARA, *J. Appl. Electrochem.* **7**, 31 (1977).
11. T. TAKAHASHI, T. ESAKA, AND H. IWAHARA, *J. Appl. Electrochem.* **7**, 299 (1977).
12. T. TAKAHASHI, T. ESAKA, AND H. IWAHARA, *J. Appl. Electrochem.* **7**, 303 (1977).
13. H. A. HARWIG AND J. W. WEENK, *Z. Anorg. Allg. Chem.*, in press.
14. J. SCHOONMAN, *J. Solid State Chem.* **5**, 62 (1972).
15. H. A. HARWIG AND G. H. J. BROERS, to appear.
16. H. A. HARWIG, *Z. Anorg. Allg. Chem.*, in press.
17. R. E. CARTER AND W. L. ROTH, *in* "Electromotive Force Measurements in High Temperature Systems" (C. B. ALCOCK, Ed.), p. 125, Elsevier, New York (1968).
18. R. S. SETHI AND H. C. GAUR, *Indian J. Chem.* **3**, 177 (1965).
19. F. A. KRÖGER, "The Chemistry of Imperfect Crystals," Vol. 2, 2nd ed., North–Holland, Amsterdam (1974).
20. J. H. W. DE WIT, *J. Solid State Chem.* **20**, 143 (1977).